Lattice instability coupled with valence degrees of freedom in valence fluctuation compound YbPd

Satoshi Tsutsui [1,2,*] Takumi Hasegawa,[3] Akihiro Mitsuda [4] Masaki Sugishima,[5,†] Kohei Oyama,[4] Masaichiro Mizumaki,[1]
Norio Ogita,[3] Hirofumi Wada,[4] and Masayuki Udagawa [3]

[1]*Japan Synchrotron Radiation Research Institute (JASRI), SPring-8, Sayo, Hyogo 679–5198, Japan*
[2]*Institute of Quantum Beam Science, Graduate School of Science and Engineering, Ibaraki University, Hitachi, Ibaraki 316–8511, Japan*
[3]*Graduate School of Integrated Arts and Sciences, Hiroshima University, Higashi-Hiroshima, Hiroshima 739–8521, Japan*
[4]*Department of Physics, Kyushu University, Fukuoka, Fukuoka 819-0395, Japan*
[5]*Technical Division, Iwate University, Morioka, Iwate 020–8550, Japan*

Inelastic x-ray scattering (IXS) was used to examine the valence fluctuation compound YbPd at 300 K in the Γ-X, Γ-M, X-M, and X-R directions. The obtained spectra and determined phonon dispersion relations demonstrate lattice instabilities related to the successive transitions and correlations between phonon spectra and valence degrees of freedom in YbPd. The low-lying branches in the phonon dispersion relations as well as the broadened linewidths of the IXS spectra observed around the longitudinal X point provide supporting evidence of correlation between a valence-lattice interaction and the successive transitions in YbPd. X-ray absorption spectroscopy was also performed in order to discuss correlations between lattice instabilities and Yb valence degrees of freedom in YbPd.

I. INTRODUCTION

YbPd undergoes successive transitions based on multiple degrees of freedom in spite of its simple crystal structure. YbPd has a CsCl-type crystal structure at room temperature that is isostructural with the other RPd (R: rare earth) [1]. Judging from the rare-earth dependence of the lattice constant in RPd, the valence state of Yb ions in YbPd is between the divalent and trivalent states. YbPd has at least four phase transitions at low temperatures [2]. A transition from a phase with cubic symmetry to that with tetragonal symmetry at a low temperature was revealed by x-ray diffraction [3]. At least one of these transitions at lower temperatures below 1.7 K is a magnetic transition, as suggested from the results of previous [170]Yb Mössbauer spectroscopy [3] and recent neutron diffraction [4] investigations.

Valence degrees of freedom sometimes affect structural instabilities in materials. Intermediate valence states in some compounds undergo charge ordering accompanied by structural transition. As mentioned above, the lattice constant in the series of RPd does not obey the lanthanide contraction at YbPd, suggesting an intermediate Yb valence state [1]. The temperature dependence of the lattice constant in YbPd is weaker than those in TmPd and LuPd, suggesting temperature dependence of the Yb valence based on lanthanide contraction. A fluctuating Yb valence state was suggested from the results of Yb L_{III}-edge x-ray absorption spectroscopy (XAS) and [170]Yb Mössbauer spectroscopy [2,3]. The former

demonstrated that the Yb has a mixed valence state. The latter demonstrated that the spectrum at 4.2 K consists of a single line, suggesting a single valence state. As was discussed in Refs. [5,6], the discrepancy between the results obtained by XAS and Mössbauer spectroscopy evidences that the rare-earth valence state is fluctuating in rare-earth based intermetallic compounds such as Eu and Yb compounds [7–11]. The [170]Yb Mössbauer spectrum at 0.05 K consists of magnetic and nonmagnetic components [3], which suggests valence ordering resulting in two valence states.

Valence ordering reduces a crystallographic symmetry because of the difference in ionic radius. Some experimental results indicate the presence of structural transitions in YbPd. As mentioned above, the transition from a structure with cubic symmetry to that with tetragonal symmetry was first observed in an x-ray diffraction experiment [3]. A Raman scattering experiment demonstrated structural transitions above 100 K that support the results of the previous x-ray diffraction experiment [12]. More precise crystallographic studies of YbPd in reciprocal spaces have recently been performed by x-ray diffraction [13–15]. The obtained results demonstrated that the successive transitions above 100 K are caused by structural transitions. A structural transition from a cubic phase to a tetragonal one occurs at $T_1 = 125$ K [13]. Yb atoms occupy nonequivalent crystallographic sites below $T_2 = 105$ K [13,14]. Successive incommensurate-commensurate transitions occur at these temperatures [15]. These experimental findings imply that structural instabilities are correlated with Yb valence degrees of freedom in YbPd.

The first investigation of lattice dynamics related to a possible valence ordering was performed for YbPd via inelastic x-ray scattering (IXS) [16]. Softening around the x point along the longitudinal (1 0 0) direction [$X(L)$ point] was found

---

*satoshi@jasri.jp
†Present address: National Institutes for Quantum and Radiological Science and Technology, Takasaki, Gunma 370–1292, Japan.

245150-1

at 300 K. Since the X point corresponds to cell doubling due to nonequivalent crystallographic Yb sites, this softening suggests coupling between the Yb valence and the structural instability in YbPd. In addition, broadened spectra were observed near the zone boundary of the longitudinal (1 0 0) direction in spite of the absence of any softening or broadening in the transverse (1 0 0) direction. This also implies that the anomalies observed in only the longitudinal (1 0 0) direction correlate with the valence degrees of freedom in the valence fluctuation system of YbPd. However, the flat dispersion and broadened linewidth of the acoustic mode near the $X(L)$ point are anomalous in conventional charge-density wave (CDW) systems [17,18]. Since the broadening is also observed in steep dispersions, the confirmation of the origin of the line broadening is required. In addition, the observation of such low-energy excitation exhibiting a flat dispersion in a certain volume of reciprocal space might affect the phonon density of states (DOS) in YbPd. In fact, an anomalous quasielastic contribution in the low-energy region was observed by inelastic neutron scattering (INS) even at a high temperature [19]. Since the interpretation of the previous INS work is based on the assumption that YbPd is isostructural with LuPd, a more precise investigation related to low-energy phonons is crucial to understand such anomalous low-energy excitations.

A calculation for YbPd based on the assumption that YbPd isostructural with LuPd was also performed [20]. Since the calculation for LuPd demonstrates the absence of softened modes at the $X(L)$ point, the softened acoustic mode observed in YbPd correlates with the Yb valence degrees of freedom. The calculation also gives a possible interpretation of the phonon dispersion relation in the Γ-$X(L)$ and IXS spectra around the $X(L)$ point based on a valence-lattice interaction. On the other hand, the calculated results indicate that softened modes exist in the X-R and X-M directions. Judging from a recent x-ray diffraction experiment [15], the softened mode in the X-R direction correlates with the incommensurate structural transition at T_1. Furthermore, the calculated results imply that the origin of the softening in the X-R direction differs from those at the $X(L)$ point and in the X-M direction: the observation of the softened mode in the X-R direction is independent of the valence-lattice interaction; the observation of the softened modes at the $X(L)$ point and in the X-M direction is independent of the valence-lattice interaction.

In this work, phonon dispersion relations were reexamined by IXS. A series of IXS experiments successfully confirmed the flat dispersion relation around the $X(L)$ point and the correlation between the softened modes and the incommensurate transition in the X-M and X-R directions. In addition, unexpected low-energy phonon contributions and the $\boldsymbol{q}$-dependent linewidth of the softened modes in the X-M and X-R directions were observed in IXS experiments. In particular, since the softened mode spectrum at the $X(L)$ point exhibits temperature dependence, correlations between the softened modes and the Yb valence are also discussed in this paper. Furthermore, Yb L_{III}-edge XAS was also performed to elucidate the relationships between structural instability and the Yb valence degrees of freedom. The combination of IXS and Yb L_{III}-edge XAS makes it possible to discuss the role of lattice instabilities and Yb valence degrees of freedom in the successive transitions of YbPd.

II. EXPERIMENTAL PROCEDURE

A. Sample preparation

Single-crystalline samples of YbPd were grown by the Yb self-flux method [13]. The size of the samples was about $1 \, \mathrm{mm}^3$. The rocking curve width was about $0.5°$ at the (4 0 0) reflection in each sample, which was large but smaller than the uncertainty owing to the $\boldsymbol{Q}$ resolution in IXS measurements, judging from the lattice constant of YbPd [1].

Polycrystalline samples of YbPd for the XAS measurements were synthesized by annealing a mixture of Yb_5Pd_2 and Pd powder samples in H_2 gas atmosphere at 923 K for 4 d [4]. Although it is difficult to crush single-crystalline YbPd samples into powder ones, this method enabled us to obtain powder YbPd samples for XAS measurements. After annealing, x-ray diffraction pattern was taken at 300 K in order to check the presence of impurity phases. The powder sample is contaminated by 11.4 wt % of Yb_2O_3 and 8.3 wt % of YbH_2, which means that 14.7 mol % of Yb^{3+} and 12.1 mol % of Yb^{2+} are contained as temperature-independent valence states in the powder sample.

B. Experimental setup of IXS

An IXS experiment was carried out at BL35XU of SPring-8 [21]. 3×4 analyzer arrays were installed in the IXS spectrometer of BL35XU. We chose the Si(11 11 11) backscattering setup: the incident x-ray energy was 21.747 keV and the energy resolution was about 1.5 meV, slightly depending on the analyzer. The typical background rate was less than 1/100 counts per second. In the present work, the $\boldsymbol{Q}$ resolutions in the IXS measurements were $\Delta \boldsymbol{Q} \sim$(0.05 0.03 0.04) in reciprocal lattice unit (r. l. u.) in the "normal" setup and $\Delta \boldsymbol{Q} \sim$(0.02 0.02 0.01) (r. l. u.) in the "high-resolution" setup, slightly depending on the scanning $\boldsymbol{Q}$ direction.

C. Experimental setup of XAS

The XAS experiment at the Yb L_{III} edge was performed at BL01B1 of SPring-8. The beam lines were composed of a double-crystal monochromator equipped with a Si(1 1 1) crystal and a Si mirror for eliminating the higher harmonics [22]. The XAS spectra were taken as the transmission ratio of x rays in the polycrystalline powder YbPd sample. The energy resolution was about 1 eV around the Yb L_{III} edge. The incident photon energy was calibrated by Yb L_{III}-edge XAS spectrum of Yb_2O_3 at 300 K.

III. EXPERIMENTAL RESULTS

A. IXS spectra in Γ-$X(L)$ with high-Q resolution

IXS spectra along the Γ-X and Γ-M directions were reported previously [16]. The spectra in both the transverse Γ-X [Γ-$X(T)$] and Γ-M [Γ-$M(T)$] directions consist of only an acoustic excitation whose energy propagates with increasing momentum transfer. In a CsCl-type structure, only an acoustic mode, whose energy increases monotonically with increasing momentum transfer in a reduced Brillouin zone, is expected around relatively strong reflections in high-symmetry directions. In this sense, the spectra in the longitudinal Γ-M [Γ-$M(L)$] direction are expected to consist of more than
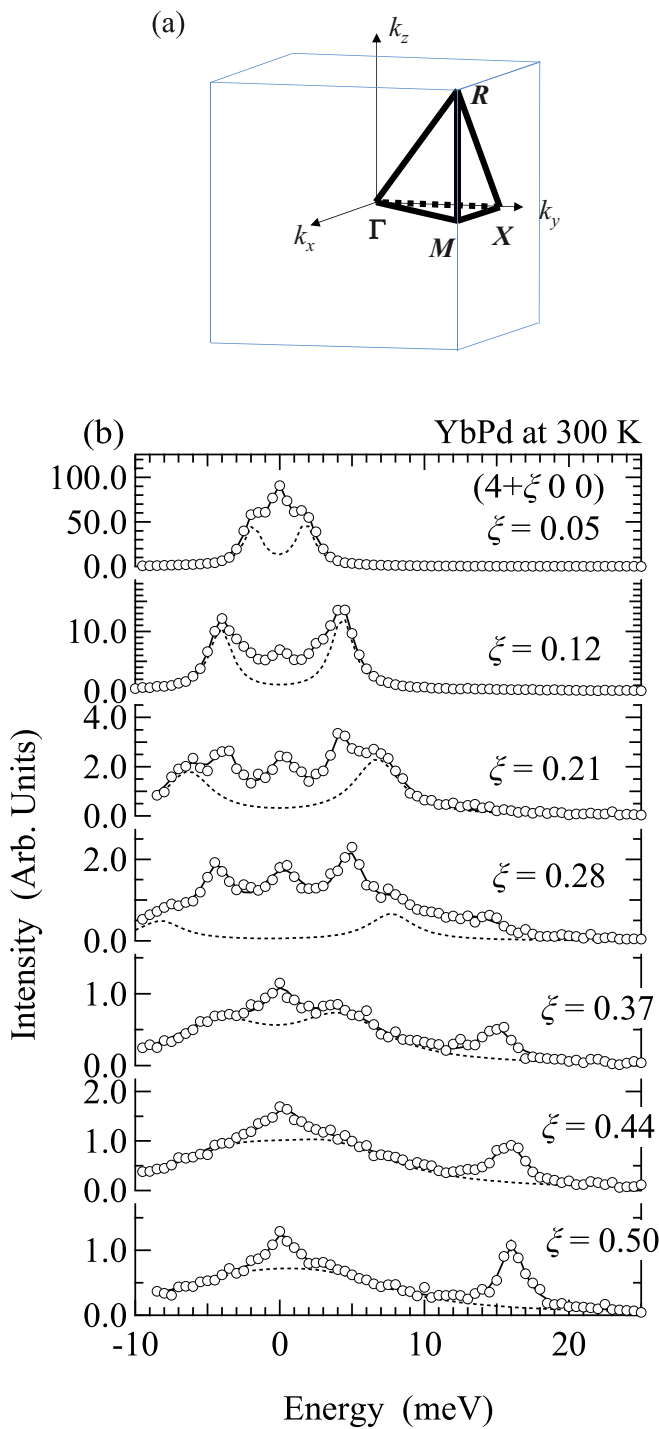
FIG. 1. (a) Brillouin zone of a CsCl-type structure isostructural with YbPd. (b) IXS spectra of YbPd taken with high-resolution setup along the Γ-$X(L)$ direction at 300 K. Open circles depict experimental data. Dashed curves depict contributions of the longitudinal acoustic modes.

sion relation observed in the Γ-$X(L)$ direction is anomalous. While a phonon mode exhibits a minimum around a certain reciprocal point in typical CDW compounds, where a superlattice reflection is found below their transition temperature [17,18], the momentum transfer dependence of the IXS spectrum along the Γ-$X(L)$ direction indicates the presence of a nearly flat dispersion around the $X(L)$ point.

Figure 1 shows the q dependence of the IXS spectrum in the Γ-$X(L)$ direction of YbPd obtained from a single-crystalline sample, where the measurements were carried out with Q resolutions higher than those in a previous work [16]. The measurements in the present work were performed with a high-resolution setup, whereas those in the previous work were performed with a normal setup. The results obtained in the present work agree with those in the previous work [16]. This indicates that the softened acoustic mode and its broadened linewidth at the $X(L)$ point are independent of the sample. Figure 2 also demonstrates the reproducibility of the phonon dispersion relation regardless of the Q resolution. The observation of the broadened spectra is also independent of the Q resolution. Since the broadening of the spectral linewidth is independent of the Q resolutions in the IXS measurements with higher Q resolution, this broadening is not caused by the phonon dispersion relation, which is sometimes observed in the measurement of spectra along steep dispersions such as acoustic modes because an effect of the slope in the phonon branch against momentum transfer includes observed linewidth of a phonon excitation at a certain Q position on the branch, but by spectral broadening unrelated to the experimental setup. In addition, since cell doubling due to valence ordering was reported previously [13,15], the softening of the acoustic mode is related to structural instability owing to valence ordering in YbPd. As mentioned above, both a plateau in the dispersion relation and broadened spectra are observed around the X(L) point. This indicates a correlation between the linewidth of the spectrum and its dispersion relation.
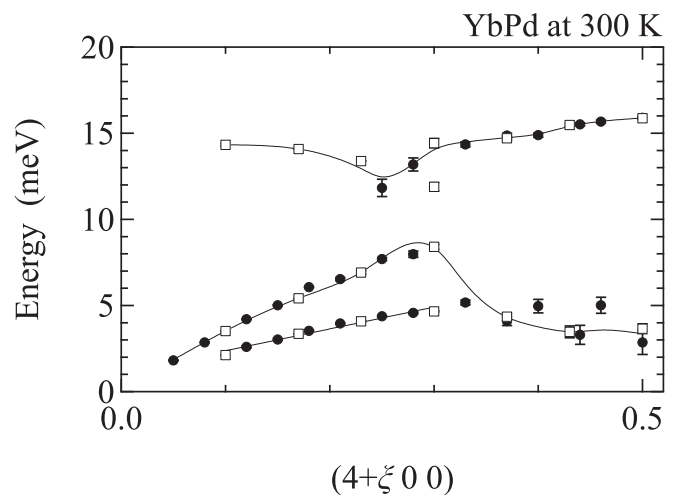

FIG. 2. Phonon dispersion relation of YbPd taken in the Brillouin zone of $(4+\xi\ 0\ 0)$ at 300 K. Closed circles (open squares) depict the data taken with the high-resolution (normal) setup. Solid curves are guides to the eye.
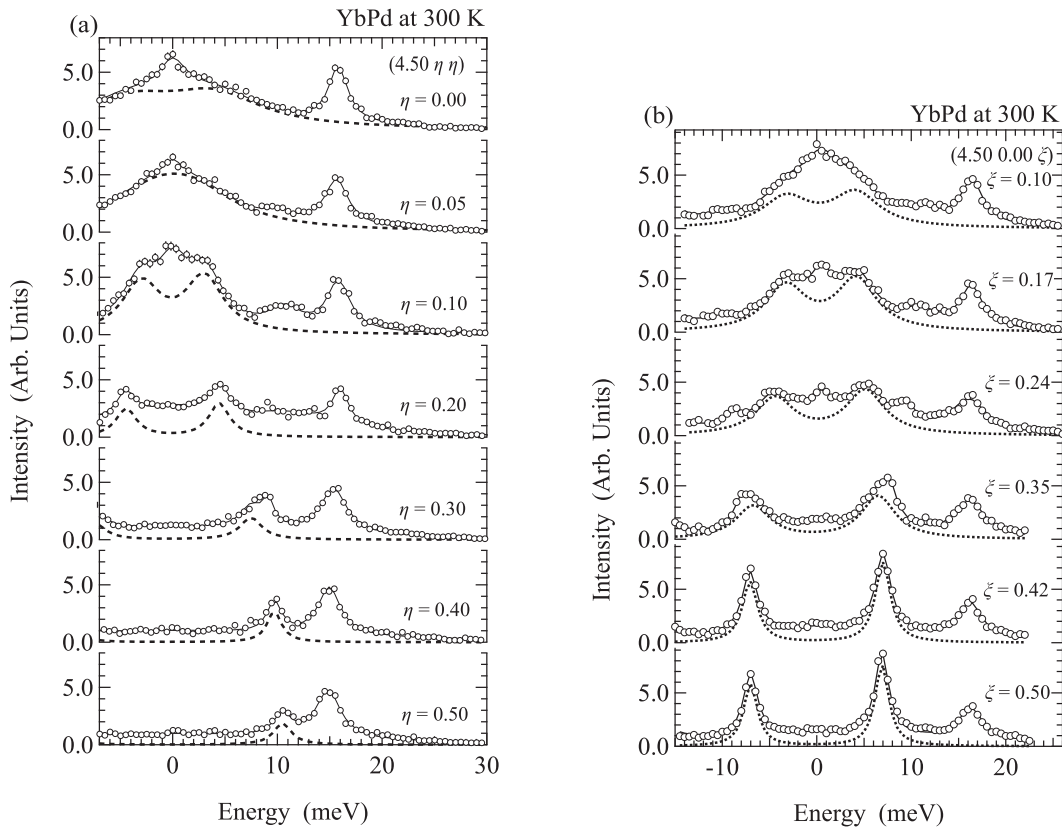
one mode near the Γ point. In addition, the excitation peak suddenly broadens near the $X(L)$ point. Simultaneously, the excitation energy also suddenly decreases near the $X(L)$ point. This was interpreted as the softening of the acoustic mode along the Γ-$X(L)$ direction. Compared with the well-known phonon dispersion relations in CDW compounds, the disper-

FIG. 3. IXS spectra of YbPd at 300 K taken with the normal setup along the (a) X(L)-R and (b) X(L)-M directions. Open circles depict experimental data. Dashed curves depict the contribution of the lowest modes in each direction.

B. IXS spectra in X(L)-R and X(L)-M directions

IXS spectra along the $X(L)$-R and $X(L)$-M directions are shown in Fig. 3. All the spectra were measured with the $\boldsymbol{Q}$ resolution in the normal setup of $\Delta\boldsymbol{Q} = (0.05\,0.03\,0.04)$ (r. l. u.). The spectra in the low-energy region consist of a broad quasielastic peak and a low-lying mode, depicted by dotted curves in Fig. 3, in both directions. The linewidth of the low-lying mode is much broader than those of the other optical modes. The low-lying contribution merges with a higher optical mode towards the R and M points. Simultaneously, the linewidth of the low-lying mode becomes increasingly narrow towards the R and M points. A quasielastic contribution is also clearly observed at the R and M points, to which assigning a mode based on the reported calculation is difficult [20]. Unknown low-lying contributions are also observed in the $X(L)$-R and $X(L)$-M directions as shown in Fig. 3. Since the reported Raman-scattering experiments imply the absence of a reduced structural symmetry from the CsCl-type crystal structure of YbPd, the observed low-lying contribution probably originated from quasielastic contributions based on electronic scattering [12].

The low-lying modes except for the quasielastic contributions are in principle related to the lattice instabilities in YbPd. In the $X(L)$-R direction, the low-lying mode exhibits a minimum around $\boldsymbol{Q} = (4.5\,0.05\,0.05)$ as shown in Fig. 3(a). The minimum phonon energy at this $\boldsymbol{Q}$ position demonstrates the lattice instability related to the incommensurate structural transition [15]. Moreover, in the $X(L)$-M direction, the linewidth of the low-lying mode becomes narrower where the

low-lying mode merges with the higher optical mode, which is similar to the low-lying mode in the $X(L)$-R direction, as shown in Fig. 3(b). The phonon energy does not exhibit a minimum between the $X(L)$ and M points but gradually increases from the $X(L)$ point to the M point, since this direction is independent of the successive structural transitions reported previously [13,15].

C. Phonon dispersion relation at 300 K

Phonon dispersion relations of R-X-Γ-M-X at 300 K are shown in Fig. 4. Most of the branches are found in YbPd. Some branches in the Γ-M and X-R directions are missing in the present work despite measuring the IXS spectra in various Brillouin zones. The LA mode in the Γ-$X(L)$ direction is softened towards the $X(L)$ point. Although the cell doubling observed in diffraction experiments indicates a dispersion relation in typical CDW transitions [13,15,17,18], the nearly flat dispersion relation observed in YbPd differs from the dispersion relations in typical CDW compounds. In addition, low-lying branches are found around the $X(L)$ point. Although the quasielastic contribution mentioned above is excluded from the dispersion relation shown in Fig. 4, low-lying modes are observed at about 3 meV around the $X(L)$ point. Such a nearly flat dispersion relation near the X point in the $X(L)$-R direction implies the competition between the instabilities related to the successive commensurate-incommensurate structural transitions [15]. Such nearly flat dispersions near the $X(L)$ position are also observed in the Γ-$X(L)$ and $X(L)$-
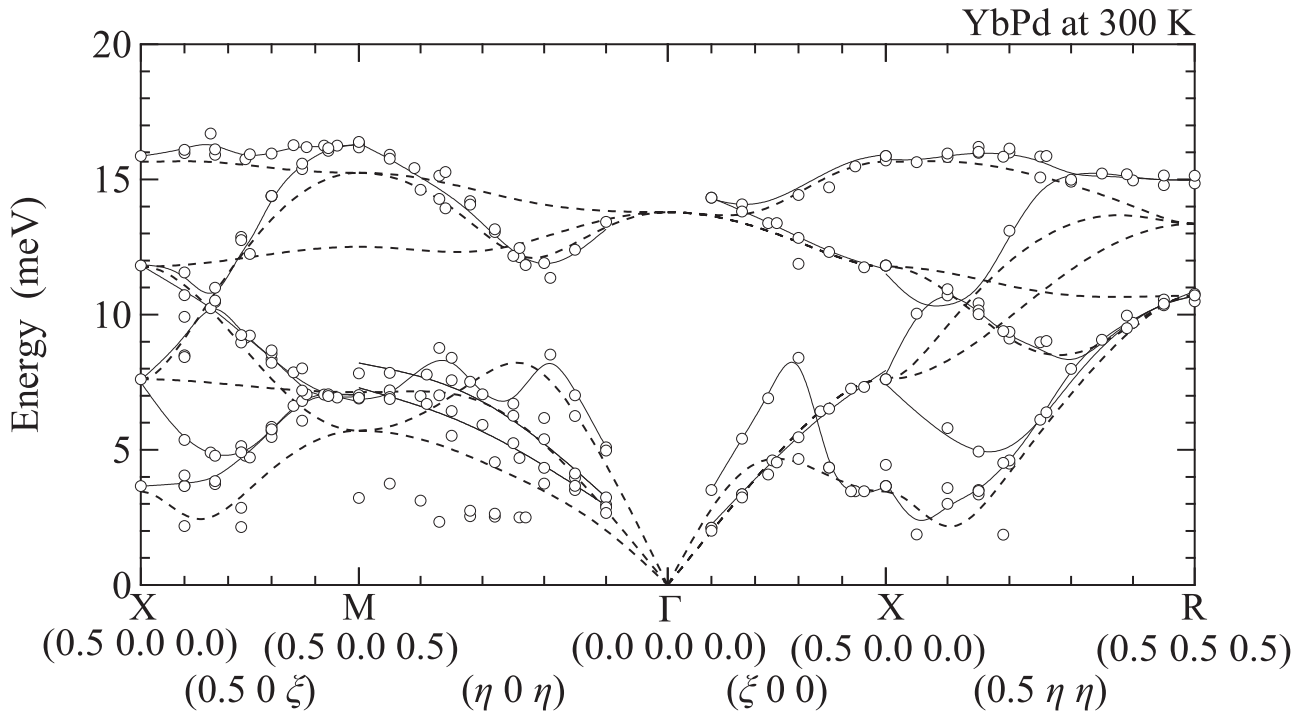
FIG. 4. Phonon dispersion relations of YbPd at 300 K. Open circles are data points obtained by IXS. Solid curves are guides to the eye. Dashed curves are the calculated results reported in Ref. [20].

M directions. This is also unexpected for CDW compounds [17,18] but agrees with theoretical findings [20].

D. Phonon excitation energy and linewidth in the Γ-$X(L)$, $X(L)$-R and $X(L)$-M directions at 300 K

Figure 5 shows the momentum transfer dependence of the phonon excitation energy and linewidth of the low-lying branches, which are denoted as dotted curves in Figs. 1 and 3, in the Γ-$X(L)$, $X(L)$-R, and $X(L)$-M directions at 300 K. Line broadening due to the $\boldsymbol{Q}$-resolution effect was not considered in these plots. These plots also exclude quasielastic contributions, and clearly demonstrate that the linewidth is extremely broad at the $X(L)$ point. The observed linewidth is nearly independent of the phonon excitation energy. In the Γ-$X(L)$, $X(L)$-M, and $X(L)$-R directions, the observed linewidth
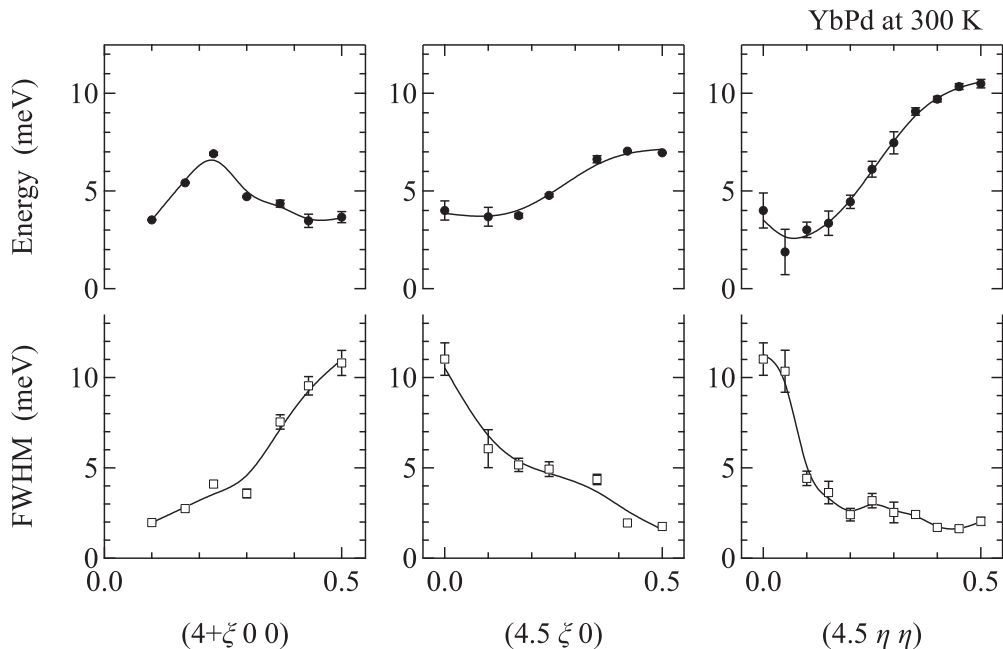

FIG. 5. Phonon dispersion relations (upper panel) and excitation linewidths (lower panel) in various directions around (4.5 0 0) at 300 K. Solid curves are guides to the eye.
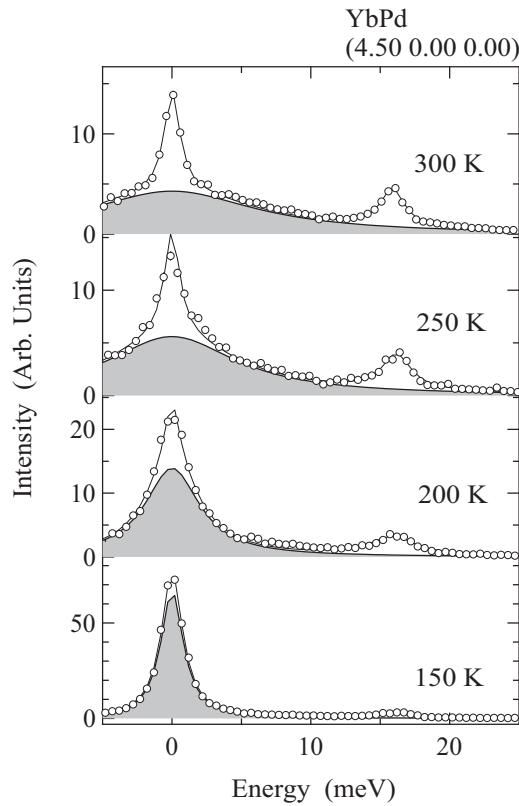
FIG. 6. Temperature dependence of the IXS spectra of YbPd at the $X(L)$ point of (4.50 0.00 0.00). The gray regions correspond to the elastic contribution at each temperature.

rapidly decreases away from the $X(L)$ point. The linewidth is nearly equal to that at $\boldsymbol{Q} = (4.5\,0.05\,0.05)$, corresponding to the $\boldsymbol{Q}$ position where the superlattice reflection due to the incommensurate transition is observed. Slight broadening is found in the middle of the branches in the $X(L)$-M and $X(L)$-R directions. This is probably caused by the line broadening due to a slope effect related to the effect of the $\boldsymbol{Q}$ resolution. In most cases, the line broadening in phonon excitations is related to the lifetime of phonons. In fact, a valence-lattice *interaction* has been predicted theoretically [20]. The results in the present work demonstrate that the observed line broadening provides supporting evidence for the presence of the valence-lattice interaction predicted previously. It also implies that the observed lattice instabilities correlate with Yb valence fluctuation.

E. Temperature dependence of IXS spectra at the $X(L)$ point

IXS spectra measured at $\boldsymbol{Q} = (4.5\,0.0\,0.0)$ exhibit temperature dependence as shown in Fig. 6. The gray component shown in Fig. 6 originates from the softened longitudinal acoustic excitation. This behaves similarly to a quasielastic excitation, whose linewidth decreases with decreasing temperature toward T_1. The temperature dependence of the linewidth is shown in Fig. 7. The linewidth approaches the resolution of the Si(11 11 11) optics at BL35XU of SPring-8. Given that YbPd is a CDW compound, such temperature dependence of the linewidth as well as a flat branch in a wide-$\boldsymbol{Q}$
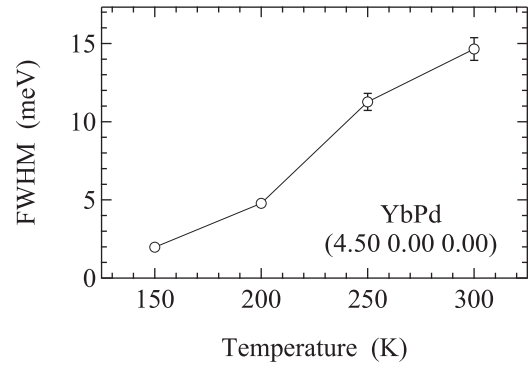

FIG. 7. Temperature dependence of the quasielastic linewidth at the $X(L)$ point of (4.50 0.00 0.00).

region near the $X(L)$ point in the dispersion relation is rare for conventional CDW compounds.

F. Yb L_{III}-edge x-ray absorption spectroscopy

The x-ray absorption spectrum of YbPd at 300 K is shown in Fig. 8. This spectrum consists of two components corresponding to divalent and trivalent states of Yb ions. This agrees with the results reported previously [2]. The average valence states estimated from the x-ray absorption spectrum are set as the intensity ratios between Yb^{2+} and Yb^{3+} components in Yb L_{III}-edge XAS. Temperature dependence of the x-ray absorption spectrum was investigated to elucidate the temperature dependence of the average Yb valence state in YbPd. The intensity ratio between the Yb^{2+} and Yb^{3+} components in the x-ray absorption spectra exhibits the temperature dependence. Meanwhile the impurities of YbH_2 and Yb_2O_3 were included in the polycrystalline powder YbPd sample. Since the Yb valence state in YbH_2 (Yb_2O_3) is divalent (trivalent) and independent of temperature, average Yb valence state obtained from the spectra was corrected by

$$V_{\mathrm{YbPd}} = \frac{V_{obs} - (2 \times R_{\mathrm{Yb2+}} + 3 \times R_{\mathrm{Yb3+}})}{1 - R_{\mathrm{Yb2+}} - R_{\mathrm{Yb3+}}}, \quad (1)$$

where V_{YbPd} is estimated Yb valence in YbPd, V_{obs} is average Yb valence estimated from the observed x-ray absorption spectra, and $R_{\mathrm{Yb2+}}$ ($R_{\mathrm{Yb3+}}$) is the ratio of the Yb^{2+} (Yb^{3+})
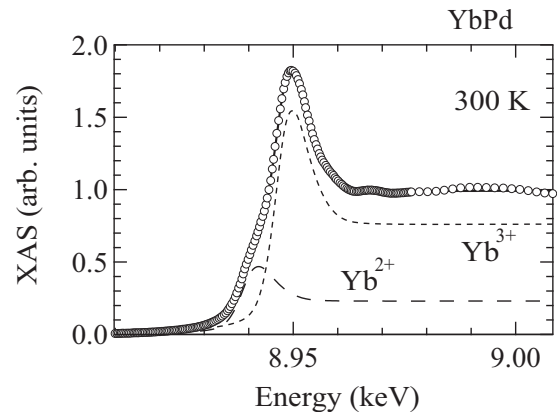

FIG. 8. Yb L_{III}-edge x-ray absorption spectrum of YbPd at 300 K.
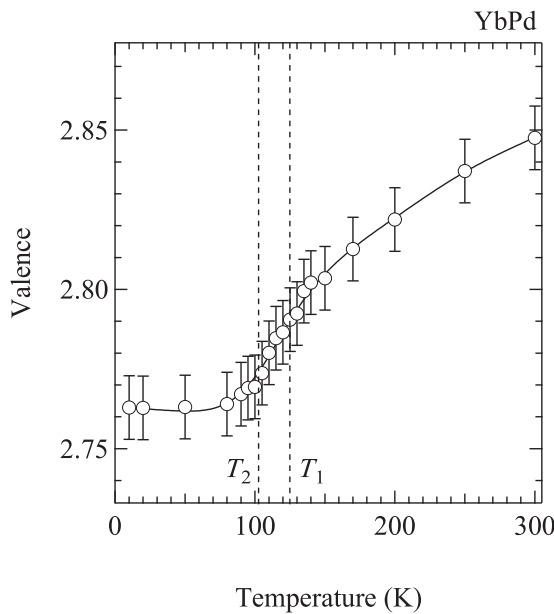
FIG. 9. Temperature dependence of average Yb valence in YbPd estimated from the Yb $L_{\rm III}$-edge x-ray absorption spectra.

impurity phase in the sample estimated from the x-ray-diffraction pattern at 300 K. Temperature dependence of the average Yb valence state estimated from XAS spectroscopy is shown in Fig. 9. The average Yb valence gradually changes from 2.85 ± 0.01 to 2.76 ± 0.01 with decreasing temperature. The change observed in the present work demonstrates that hybridization between Yb-$4f$ and Pd-$4d$ electrons strengthens with decreasing temperature.

IV. DISCUSSION

A. Lattice instability related to successive transitions

The phonon dispersion relations demonstrate the softening of the branches along the Γ-$X(L)$ and $X(L)$-R directions as shown in Fig. 5. The former is related to the commensurate structural transition whose superlattice reflection is observed at the X point of (0.5 0 0). The latter is related to the incommensurate structural transition whose superlattice reflection is observed at $\boldsymbol{q} = (0.5\,0.05\,0.05)$. In addition, the phonon excitation energy around $\boldsymbol{q} = (0.5\,0.05\,0.05)$ is lower than that at the X point. This means that the lattice instability near $\boldsymbol{q} = (0.5\,0.05\,0.05)$, corresponding to the superlattice position of the incommensurate structural transition, is higher than that at the X point. In fact, the temperature of the incommensurate structural transition is higher than that of the commensurate structural transition [15]. The present results demonstrate that the two successive transitions observed in the previous diffraction experiment [15] are both caused by the lattice instabilities.

The results obtained in the present work clearly indicate correlations between the lattice instabilities around the $X(L)$ point and successive transitions in YbPd, but the nearly flat dispersion relation in the Γ-$X(L)$ direction is anomalous from the viewpoint of conventional CDW compounds. There are several reasons for observing such a flat dispersion relation

around $X(L)$ points. One is the competition between instabilities accompanied by the commensurate and incommensurate structural transitions. Another is the effect accompanying by the valence-lattice interaction as was discussed in Ref. [20]. The other is based on instrumentation differences between IXS and INS. The two former cases will be discussed in later sections. Here, the possible effects of instrumentation differences are considered. Although both IXS and INS are techniques to investigate the phonon dispersion relations of materials as a dynamical structure factor, the relationship between momentum and energy transfer is completely different between these techniques. The relationship between energy and momentum transfer in IXS is given as

$$\boldsymbol{Q} = 2\boldsymbol{k}_f \sin \theta, \tag{2}$$

whereas that in INS is

$$\Delta E = \frac{\hbar^2}{m_n}(2\boldsymbol{k}_f - \boldsymbol{Q}) \cdot \boldsymbol{Q} \tag{3}$$

for neutrons, where ΔE, $\boldsymbol{Q}$, $\boldsymbol{k}_f$, and m_n represent the energy transfer, the momentum transfer, the momentum of an x ray, or neutron after scattering and the mass of a neutron, respectively. These equations mean that momentum transfer is decoupled (coupled) with energy transfer in x-rays (neutrons) in the scattering process. Equations (2) and (3) imply that different dynamical structure factors are observed between IXS and INS. However, the insensitivity of the obtained phonon dispersion relations to the $\boldsymbol{Q}$ resolution in the present work demonstrates that the results obtained in the present work are not also caused by an instrumental difference between IXS and INS. In fact, although a few investigations of the lattice dynamics observed in CDW compounds by performing both IXS and INS experiments have been reported, the lattice dynamics in α-U is one of the cases in the CDW compounds [23,24]. The results obtained by both IXS and INS are in agreement with the α-U case, although the momentum and energy resolutions are different between IXS and INS experiments. In the present case, we carried out a series of IXS experiments on the same sample with different momentum resolutions instead of using different techniques such as IXS and INS, and the results obtained with different momentum resolutions were identical. This means that the results obtained in the present work are unrelated to instrument effects causing a difference between IXS and INS in typical CDW compounds.

B. Correlations between line broadening of low-lying modes and lattice instabilities

We successfully found low-lying branches in the Γ-X, X-R, and X-M directions of YbPd as shown in Fig. 4. The lowest branch in the Γ-$X(L)$-R direction indicates competition between lattice instabilities accompanying by the commensurate and incommensurate structural transitions. Both softened excitation and its line broadening were observed simultaneously at the $\boldsymbol{Q}$ positions, where observation of superlattice reflections in the Γ-$X(L)$-R direction was expected such as $\boldsymbol{q} = (0.50\,0.00\,0.00)$ and $(0.50\,0.05\,0.05)$, as shown in Fig. 5.

It was found by calculation reported in Ref. [20] that another softened branch exists in the *X-M* direction. This branch exhibits a minimum at $\boldsymbol{q} = (0.50\,0.10\,0.00)$, which is similar to that in the *X(L)-R* direction. This also agrees with the calculation reported in Ref. [20]. However, no line broadening was observed at $\boldsymbol{q} = (0.50\,0.10\,0.00)$, unlike that in the Γ-*X(L)-R* direction, because the linewidth rapidly decreases from the *X(L)* and *R* points. If the line broadening of all the phonon branches observed in YbPd is caused by the valence-lattice interaction, the results shown in Figs. 5 and 6 demonstrate that the lattice instabilities in YbPd are assisted by the valence-lattice interaction suggested by the calculation, which was not considered in the calculation [20].

In addition, the IXS spectra obtained in the Γ-*M-X* direction are difficult to fit only with allowed phonon excitations in a CsCl-type structure because of a kind of broad background near the elastic peak as reported previously [16]. The total number of phonon branches is in principle determined by the crystal structure. YbPd has six allowed phonon branches at 300 K because it is a CsCl-type crystal structure. To sufficiently fit the spectra reported previously [16], additional broad and low-lying excitations are required as shown in Fig. 4. The contribution of additional low-lying and broad excitations around 3 meV is required to fit the IXS spectra in the Γ-*X-M* direction. The linewidth of these excitations is much broader than the resolution determined by the Si(11 11 11) setup at BL35XU of SPring-8. Such an effect was not expected in the calculation [20]. This effect is possibly caused by another valence-lattice interaction and/or Yb valence fluctuation because incident x rays directly interact with electrons in x-ray scattering processes. In addition, since the reported results of Raman scattering support the absence of symmetry breaking from a CsCl-type structure [12], the additional components observed in the Γ-*X-M* directions do not infer intrinsic phonon excitation but quasielastic scattering possibly involving electronic scattering such as valence fluctuation.

Moreover, hybridization between the Yb-4f and Pd-4d electrons, which was suggested by the results of point-contact spectroscopy [25], was not considered in the calculation in Ref. [20]. This is supported by the temperature dependence of the average Yb valence state as shown in Fig. 9, implying hybridization between 4f and conduction electrons and its temperature dependence. The role of hybridization between rare-earth 4f and Pd-4d electrons in the valence fluctuation of rare-earth atoms was discussed previously for $Eu_3Pd_{20}Ge_6$ [26]. The discrepancy between the experimental results in the present work and the calculated results such as the broad and low-lying excitations in the Γ-*X-M* direction might have been caused by the absence of hybridization between Yb-4f and Pd-4d electrons. According to the calculation in Ref. [20], the interatomic interaction between nearest-neighbor Yb atoms is stable, regardless of whether the Yb valence state is pure Yb^{2+} or Yb^{3+}, but that between nearest-neighbor Pd atoms is unstable. In this sense, the observation of the valence-lattice interaction as broadened IXS spectra is crucial for discussing the instability at the *X* point in YbPd. Concerning the interatomic interactions among the Pd atoms, the interactions between the second-nearest-neighbor Pd atoms as well as those between the nearest-neighbor Pd atoms are unstable.

This might be related to the instability corresponding to the minimum observed in the *X(L)-R* direction, but this is difficult to conclude because the valence-lattice interaction was considered to occur only along the [1 0 0] direction. Considering the temperature dependence of the Yb valence state shown in Fig. 9, the hybridization between Yb-4f and Pd-4d electrons, which was excluded in the calculation reported in Ref. [20], may affect such instabilities around the *X(L)* point in YbPd.

C. Quasielastic contribution around the *X(L)* points

The quasielastic contribution in YbPd was discussed in a previous INS experimental study [19]. This temperature dependence is anomalous, because the magnetic quasielastic contribution remains at a very high temperature. The present work provides insight to understand such an anomalous quasielastic contribution in YbPd. In the previous INS work [19], the experiment was performed with a polycrystalline sample. This means that the experimental results correspond to the generalized DOS based on the differences in the INS spectra between YbPd and LuPd. According to the experimental results obtained in the present work, a significant low-lying contribution due to phonon excitations was found around the *X(L)* point and in the *X(L)-R* and Γ-*M-X* directions. Since LuPd exhibits no structural transitions [19], no structural instabilities are expected. Therefore, a difference in phonon DOS between YbPd and LuPd can be expected. If the low-lying excitations in the Γ-*M-X* direction are an electronic contribution, this is difficult to observe in INS experiments. However, the phonon dispersion relation shown in Fig. 5 indicates a large low-energy contribution originating from low-lying phonon excitations. In addition, the temperature dependence of the IXS spectrum at the *X(L)* point as shown in Fig. 6 also supports the existence of a low-lying phonon contribution even at high temperatures, which may be observed as quasielastic contributions even in the difference of the INS spectra between YbPd and LuPd. Unlike magnon excitations, the observation of low-energy phonon excitations as a quasielastic contribution in YbPd is not anomalous and is a plausible interpretation to understand the reported quasielastic excitation at high temperatures, at least above T_1, corresponding to the temperature for the incommensurate structural transition.

The temperature dependence of the IXS spectra at the *X(L)* point is important for discussing relationships between the IXS spectra and the valence fluctuation. The Yb valence state rapidly changes near the successive structural transition temperatures as shown in Fig. 9. The temperature dependence of the elastic linewidth also decreases rapidly with decreasing temperature towards the incommensurate structural transition temperature. Since the linewidth of phonon excitations including quasielastic excitations is proportional to the inverse of the phonon lifetime, the temperature dependence might correlate with the fluctuating Yb valence state. Since the temperature dependence of the IXS spectra at the *X(L)* point differs from that of conventional CDW compounds as discussed above, one possible interpretation of the quasielastic excitation observed around the *X(L)* point is the coupling between the phonon

excitation and the Yb valence fluctuation based on the hybridization between Yb-$4f$ and Pd-$4d$ electrons in YbPd.

V. SUMMARY

Anomalous phonon dispersion relations and spectra were found in YbPd by IXS measurements. The former are related to the successive transitions observed in x-ray diffraction experiments. The dispersion relation along the Γ-$X(L)$ direction differs from those observed in typical CDW compounds. The instability at the $X(L)$ point corresponds to the commensurate structural transition. The instability along the X(L)-R direction predicted by *ab initio* calculation was found in the present work. This corresponds to the incommensurate structural transition. The broadened spectra around the $X(L)$ point are in good agreement with the calculated results, but unexpected quasielastic contributions not predicted by the calculation were also observed in some directions. The temperature dependence of the Yb valence state investigated by XAS measurements correlates with that of the quasielastic linewidth investigated by IXS measurements.

[1] A. Iandelli, G. L. Olcese, and A. Palenzona, J. Less-Common Metals **76**, 317 (1980).

[2] R. Pott, W. Boksch, G. Leson, B. Politt, H. Schmidt, A. Freimuth, K. Keulerz, J. Langen, G. Neumann, F. Oster, J. Röhler, U. Walter, P. Weidner, and D. Wohlleben, Phys. Rev. Lett. **54**, 481 (1985).

[3] P. Bonville, J. Hammann, J. A. Hodges, P. Imbert, and G. J. Jéhanno, Phys. Rev. Lett. **57**, 2733 (1986).

[4] K. Oyama, M. Sugishima, K. Tanabe, A. Mitsuda, H. Wada, K. Ohyama, T. Matsukawa, Y. Yoshida, A. Hoshikawa, T. Ishigaki, and K. Iwasa, J. Phys. Soc. Jpn. **87**, 114705 (2018).

[5] W. Kohn and T. K. Lee, Philos. Mag. A **45**, 313 (1980).

[6] S. Tsutsui, M. Mizumaki, and Y. Kobayashi, Hyperfine Interact. **240**, 84 (2019).

[7] E. Kemly, M. Croft, V. Murgai, L. C. Gupta, C. Godart, R. D. Parks, and C. U. Segre, J. Magn. Magn. Mater. **47-48**, 403 (1985).

[8] G. Wortmann, K. H. Frank, E. V. Sampathkumaran, B. Perscheid, and G. Kaindl, J. Magn. Magn. Mater. **49**, 325 (1985).

[9] G. Wortmann, I. Nowik, B. Perscheid, G. Kaindl, and I. Felner, Phys. Rev. B **43**, 5261 (1991).

[10] A. Mitsuda, H. Wada, M. Shiga, and T. Tanaka, J. Phys.: Condens. Matter. **12**, 5287 (2000).

[11] P. Bonville, C. Gondart, E. Alleno, F. Takahashi, E. Matsuoka, and M. Ishikawa, J. Phys.: Condens. Matter. **15**, L263 (2003).

[12] T. Hasegawa, N. Ogita, M. Sugishima, A. Mitsuda, H. Wada, and M. Udagawa, J. Phys.: Conf. Ser. **273**, 012030 (2011).

[13] A. Mitsuda, M. Sugishima, T. Hasegawa, S. Tsutsui, M. Isobe, Y. Ueda, M. Udagawa, and H. Wada, J. Phys. Soc. Jpn. **82**, 084712 (2013).

[14] A. Miyake, K. Kasano, T. Kagayama, K. Shimizu, R. Takahashi, Y. Wakabayashi, T. Kimura, and T. Ebihara, J. Phys. Soc. Jpn. **82**, 084706 (2013).

[15] R. Takahashi, T. Honda, A. Miyake, T. Kagayama, K. Shimizu, T. Ebihara, T. Kimura, and Y. Wakabayashi, Phys. Rev. B **88**, 054109 (2013).

[16] A. Mitsuda, M. Sugishima, T. Hasegawa, S. Tsutsui, A. Q. R. Baron, M. Udagawa, and H. Wada, JPS Conf. Proc. **3**, 011037 (2014).

[17] R. E. Peierls, *Quantum Theory of Solids* (Oxford University Press, New York, 1955).

[18] G. Grüner, *Density Waves in Solids* (Addison-Wesley, Reading, MA, 1994).

[19] U. Walter and D. Wohlleben, Phys. Rev. B **35**, 3576 (1987).

[20] T. Hasegawa, N. Ogita, A. Mitsuda, M. Sugishima, H. Wada, S. Tsutsui, and M. Udagawa, J. Phys.: Conf. Ser. **592**, 012061 (2015).

[21] A. Q. R. Baron, Y. Tanaka, S. Goto, K. Takeshita, T. Matsushita, and T. Ishikawa, J. Phys. Chem. Solids **61**, 461 (2000).

[22] T. Uruga, H. Tanida, Y. Yoneda, K. Takeshita, S. Emura, M. Takahashi, M. Harada, Y. Nishihata, Y. Kubozono, T. Tanaka, T. Yamamoto, H. Maeda, O. Kamishima, Y. Takabayashi, Y. Nakata, H. Kimura, S. Goto, and T. Ishikawa, J. Synchrotron Radiat. **6**, 143 (1999).

[23] H. G. Smith, N. Wakabayashi, W. P. Crummett, R. M. Nicklow, G. H. Lander, and E. S. Fisher, Phys. Rev. Lett. **44**, 1612 (1980).

[24] S. Raymond, J. Bouchet, G. H. Lander, M. Le Tacon, G. Garbarino, M. Hoesch, J.-P. Rueff, M. Krisch, J. C. Lashley, R. K. Schulze, and R. C. Albers, Phys. Rev. Lett. **107**, 136401 (2011).

[25] M. Shiga, K. Okimura, H. Takata, A. Mitsuda, I. Maruyama, H. Wada, Y. Inagaki, and T. Kawae, Phys. Rev. B **100**, 245117 (2019).

[26] S. Tsutsui, M. Mizumaki, Y. Kobayashi, J. Kitagawa, and T. Takabatake, Phys. Rev. B **80**, 235115 (2009).